PNAS

www.pnas.org

Supplementary Information for

Pluto near the edge of chaos

Renu Malhotra and Takashi Ito

Renu Malhotra
E-mail: malhotra@arizona.edu

This PDF file includes:

Supplementary text
Figs. S1 to S2 (not allowed for Brief Reports)
Tables S1 to S2 (not allowed for Brief Reports)
SI References

Eccentricity and inclination evolution

In the simulations of the modified restricted three body model as well the full N-body model, the time variations of the eccentricity and the inclination of Pluto-like objects are both closely related to the time variations of the argument of perihelion, ω. Figure S1 shows the time evolution of these three variables over 2 Gy for the highest fidelity N-body model, `JSUNP` (shown in blue, in the right-most panels), and for two cases of the modified restricted three body model (Sun–Neptune–Pluto, with $J_2 = 600$ and $J_2 = 1000$, shown in the left and middle panels). The latter two cases are illustrative of the range of J_2 values, 600–1300, in which a Pluto-like object's ω has chaotic behavior. In these cases we observe that the chaotic variations of the eccentricity and inclination have larger range than in the `JSUNP` system, and that the eccentricity reaches values exceeding ~ 0.3. Astronomical observations obtained thus far indicate that transneptunian objects in Neptune's 3/2 mean motion resonance are limited to eccentricities below ~ 0.3 (e.g. 1). The lower perihelion distance achieved with higher eccentricity leads to a larger destabilizing influence of closer approaches with Uranus. This explains the paucity of higher eccentricity Plutinos. This effect would be especially acute in the absence of steady latitudinal librations of the perihelion away from the plane of the planets. We therefore infer that in the regime of $600 \lesssim J_2 \lesssim 1300$, Pluto-like objects would be vulnerable to ejection from Neptune's mean motion resonance, with ensuing close approaches to the planets and eventual collision or transfer into scattered orbits or escape from the solar system.
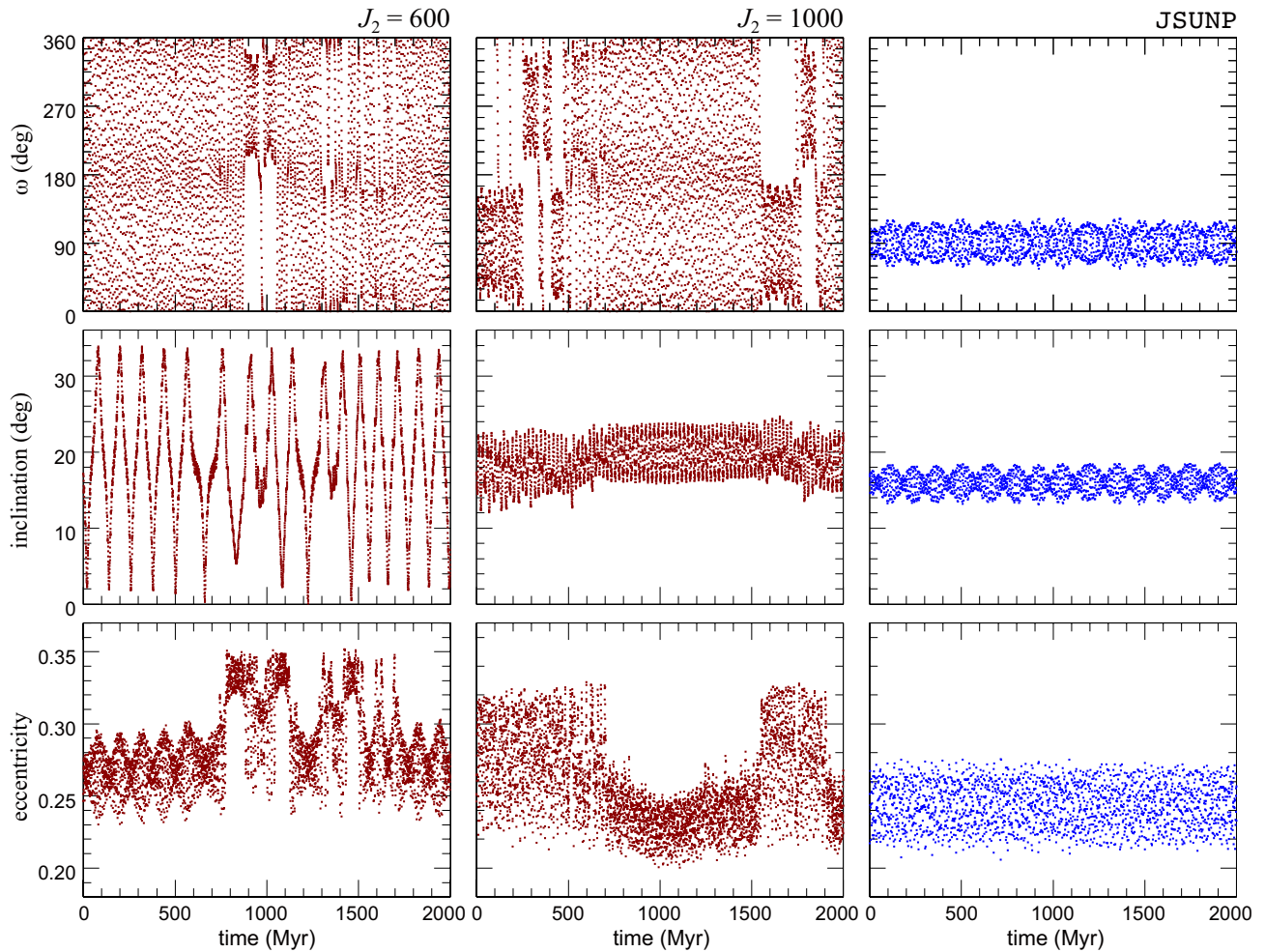

Fig. S1. Time evolution over 2 Gy of Pluto's eccentricity, inclination, and its argument of perihelion ω, in three models: (left) modified restricted three body model (Sun–Neptune–Pluto) with total effective $J_2 = 600$, (middle) modified restricted three body model with total effective $J_2 = 1000$, (right) highest fidelity N-body simulation including all four giant planets (`JSUNP`).

Effect of giant planets' migration on total effective J_2

We can see from Eq. (4) in the main text that the time history of the total effective J_2 arising from Jupiter, Saturn and Uranus will depend on the time history of the semimajor axis of each of these giant planets during their past orbital migration. Currently, these time histories are not well constrained. (In principle, the total effective J_2 also depends upon the time history of the planetary masses, but it is reasonable to assume that the planetary masses did not change significantly after their formation.) In the previous literature, the magnitudes of migration discussed are approximately a few tenths au inward migration of Jupiter, ~ 1 au outward migration of Saturn, and a few au outward migration of Uranus. With these estimates, we find that the changes in the total effective J_2 during migration would have been most sensitive to Uranus' migration. As a first quantitative estimate, we find that the total effective J_2 would have remained within the range 1350–1650 that we found for Pluto's long-term stability in its current orbit (Figure 5 in the main text), provided that the magnitude of Uranus' outward migration was less than about 5 au. An outward migration of Uranus by more than ~ 5 au would potentially change the total effective J_2 enough to transition from the latitudinal libration of Pluto's argument of perihelion being unstable to stable. We note that better estimates would take account of the effects of the more massive ancient planetesimal disk and the changes in Pluto's orbit itself during the migration of the giant planets. Further investigation of this point may provide insights into the mechanism for capturing Pluto (and many Plutinos) into the libration state of the argument of perihelion that we observe today.

Figure S2 shows the time evolution of the total effective J_2 for a simple migration model in which the planets' orbits migrate with an e-folding timescale, τ. The magnitude of each planet's migration is indicated in the figure legend.

$$\Delta a = -0.2 \text{ (J)}, +0.8 \text{ (S)}, +3.0 \text{ (U)}$$
$$\Delta a = -0.4 \text{ (J)}, +1.0 \text{ (S)}, +3.0 \text{ (U)}$$
$$\Delta a = -0.3 \text{ (J)}, +1.0 \text{ (S)}, +5.0 \text{ (U)}$$
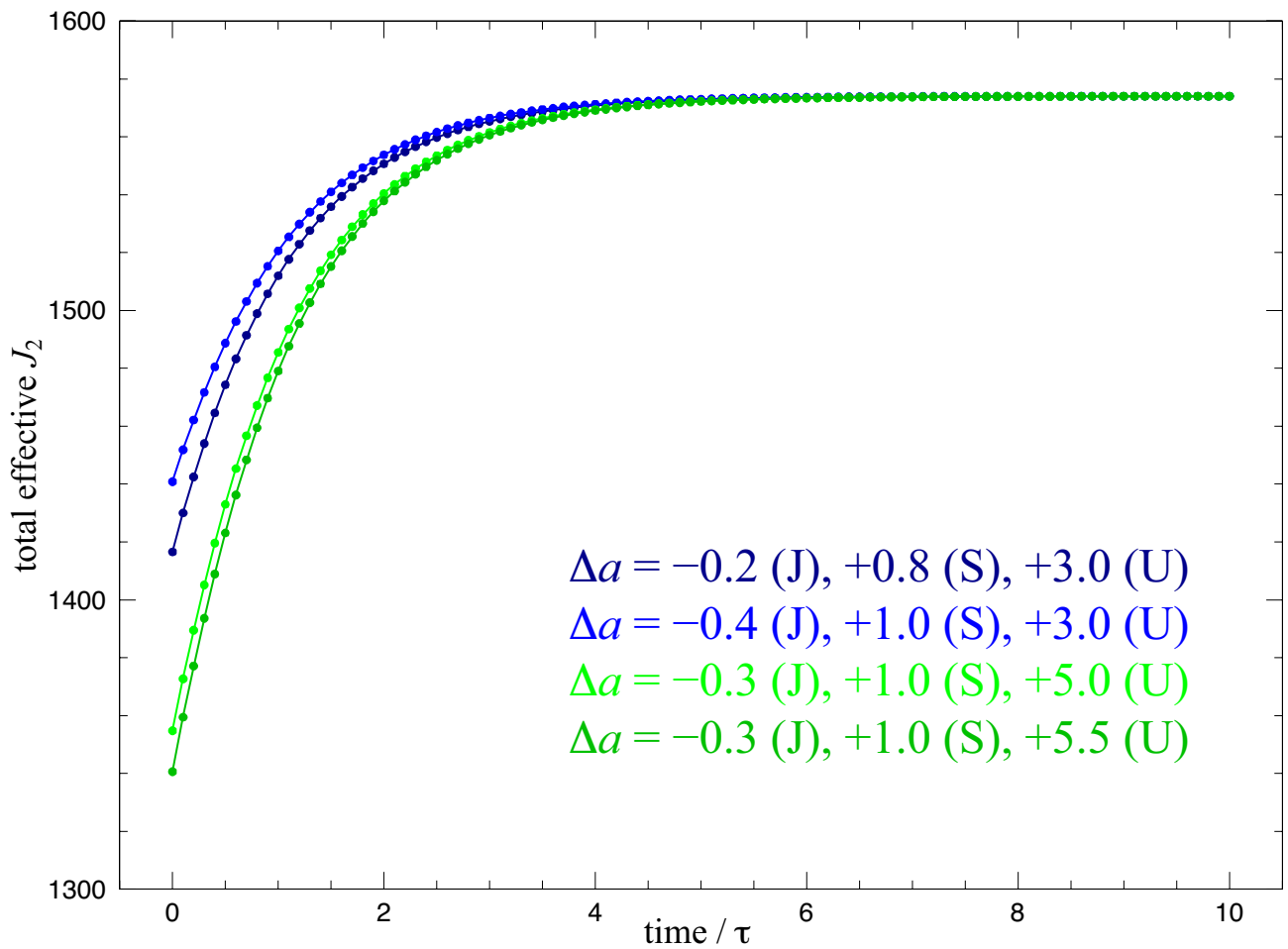$$\Delta a = -0.3 \text{ (J)}, +1.0 \text{ (S)}, +5.5 \text{ (U)}$$

Fig. S2. Time evolution of the total effective J_2 in a simple model of the orbital migration of Jupiter, Saturn and Uranus. The planets are assumed to migrate with an e-folding migration timescale, τ. The magnitude of the migration, Δa, of each planet is indicated in the legend. For example, "-0.2 (J)" means that Jupiter's semimajor axis decreases by 0.2 au; "$+5.5$ (U)" means that Uranus' semimajor axis increases by 5.5 au.

Data Availability

The data supporting this study's findings are available within the article and its Supplementary Information. Raw output data from our numerical orbit integrations is available from the authors upon reasonable request. See also Section Numerical experiments—N-body simulations in the main text for the details of the numerical integration scheme.

Location of the SWIFT code package. Access https://www.boulder.swri.edu/ hal/swift.html for retrieving the source code package.

Masses of the Sun and the planets. The masses of the Sun and the planets are listed in Table S1. The unit in this table is what is used in the SWIFT code where the gravitational constant is unity, the unit of length is au, and the unit of time is day, and one year is exactly 365.25 days. We adopted the masses of the planets from JPL's DE245 (e.g. 2). Note that Pluto is treated as a massless particle in our simulations, and it is not listed in Table S1.

Table S1. Sun's and planet's masses.

object	mass
Sun	$2.959139768995959 \quad \times 10^{-4}$
Jupiter	$2.82536279610815247 \times 10^{-7}$
Saturn	$8.45976574787474959 \times 10^{-8}$
Uranus	$1.29203489551819958 \times 10^{-8}$
Neptune	$1.52436801162357287 \times 10^{-8}$

Initial heliocentric positions and velocities of the planets and Pluto. Table S2 shows the initial heliocentric positions and velocities of the planets and Pluto in our numerical simulations that we adopted from JPL Horizons System, and they are the values as of 2021 March 19 00:00:00 TDB (Barycentric Dynamical Time). The position and the velocity of each planet are those of its barycenter (including its satellite system). Pluto's position and velocity are also those of the barycenter of the Pluto system.

Table S2. Initial positions (x, y, z) and velocities (v_x, v_y, v_z) of the planets and Pluto.

		Jupiter	
(x, y, z) au	$+3.479871576082048 \times 10^{0}$	$-3.687143487014625 \times 10^{0}$	$-6.254225671208241 \times 10^{-2}$
(v_x, v_y, v_z) au/day	$+5.402875942445465 \times 10^{-3}$	$+5.540962998223180 \times 10^{-3}$	$-1.438919301148455 \times 10^{-4}$
		Saturn	
(x, y, z) au	$+5.820837611255400 \times 10^{0}$	$-8.099314046939625 \times 10^{0}$	$-9.084726091630656 \times 10^{-2}$
(v_x, v_y, v_z) au/day	$+4.225945590475764 \times 10^{-3}$	$+3.247914368493194 \times 10^{-3}$	$-2.246007629992486 \times 10^{-4}$
		Uranus	
(x, y, z) au	$+1.515559431707809 \times 10^{1}$	$+1.268157394646391 \times 10^{1}$	$-1.492515199899297 \times 10^{-1}$
(v_x, v_y, v_z) au/day	$-2.547970714590798 \times 10^{-3}$	$+2.838524448937736 \times 10^{-3}$	$+4.340564757625335 \times 10^{-5}$
		Neptune	
(x, y, z) au	$+2.950068586930330 \times 10^{1}$	$-4.991750775881499 \times 10^{0}$	$-5.771477267043819 \times 10^{-1}$
(v_x, v_y, v_z) au/day	$+5.087496282435223 \times 10^{-4}$	$+3.120340880227267 \times 10^{-3}$	$-7.590654143371072 \times 10^{-5}$
		Pluto	
(x, y, z) au	$+1.428680876763813 \times 10^{1}$	$-3.110962891479370 \times 10^{1}$	$-8.023206165392421 \times 10^{-1}$
(v_x, v_y, v_z) au/day	$+2.933163077825810 \times 10^{-3}$	$+6.417680020238108 \times 10^{-4}$	$-9.148165866326484 \times 10^{-4}$

Values of Sun's J_2. The following values of Sun's J_2 are used for the simulations of the modified restricted three body problem whose results are summarized in Figure 5 in the main text: $J_2 = 1, 10, 100, 150, 200, 300, 400, 500, 600, 700, 800, 900, 1000, 1100, 1200, 1250, 1300, 1350, 1400, 1450, 1500, 1550, 1600, 1650, 1700, 1750, 1800, 1850, 1900, 1950, 2000, 2050, 2100, 2150, 2200, 2250, 2300, 2350, 2400, 2450, 2500, 2550, 2600, 2650, 2700, 2750, 2800, 2850, 2900, 2950, 3000, 3100, 3200, 3300, 3400, 3500, 3600, 3700, 3800, 3900, 4000, 4100, 4200, 4300, 4400, 4500, 4600, 4700, 4800, 4900, 5000, 6000, 7000,$ and 10000. The time series of ϕ and the trajectories on the $(e \cos \omega, e \sin \omega)$ plane in eight of these cases, specifically $J_2 = 100, 1000, 1350, 1500, 3000, 3100, 4000, 10000$, are plotted in Figure 4 in the main text as illustrative examples.

Specifying the J_2 values in the SWIFT code. We assumed that the solar radius is 0.00465247265886874 au. This value becomes an input to calculate the effective J_2 values used in the SWIFT code. For example when $J_2 = 1000$, we enter $1000 \times 0.00465247265886874^{2} = 0.02164550184152116$ in the `pl.in` parameter file for the SWIFT code.

References

1. B Gladman, K Volk, Transneptunian space. *Annu. Rev. Astron. Astrophys.* **59**, 203–246 (2021).
2. T Fukushima, Time ephemeris. *Astron. Astrophys.* **294**, 895–906 (1995).